Applied Radiation and Isotopes 212 (2024) 111454

Contents lists available at ScienceDirect

Applied Radiation and Isotopes

journal homepage: www.elsevier.com/locate/apradiso

Real-time gamma-ray energy spectrum / dose monitor with *k*-α method based on sequential bayesian estimation

Isao Murata *, Nikolaos Voulgaris, Takaaki Miyoshi, Moe Shinohara, Hikari Nishimura, Mina Kobayashi, Sachie Kusaka, Shingo Tamaki, Fuminobu Sato

Division of Sustainable Energy and Environmental Engineering, Graduate School of Engineering, Osaka University, Yamadaoka 2-1, Suita Osaka, Japan

ABSTRACT

Medical applications of radiation have been widely spread until now. However, the exposure of medical staff is sometimes overlooked, because treatment of patients is the first priority. The purpose of this study is to develop a small and light monitor that can measure the energy spectrum and dose of gamma-rays at the same time in real-time for medical applications. Using the monitor, the medical staff could be guided to be more aware ofthe risk of radiation, and finally the exposure to them could be substantially suppressed. So far, a CsI scintillator has been chosen as a detection device of gamma-rays and combined with a Multi-Pixel Photon Counter (MPPC) to develop a prototype monitor. Then we confirmed its basic performance with standard gamma-ray sources. To achieve the real-time measurement, α method (sequential Bayesian estimation) was adopted and improved to propose a new unfolding process, named *k*-α method, with which the convergence speed could really be accelerated to realize real-time measurement. Also, gamma-ray measurements with a mixed source of ^{133}Ba, ^{137}Cs and ^{60}Co were carried out to confirm the validity of the present monitor. As a result, it was found that gamma-ray energy spectrum could be estimated successfully in several-tens seconds in the field of around 6 μSv/h. For the dose estimation, the correct values could be estimated just after starting measurement.

1. Introduction

At present, radiation is frequently utilized for medical applications such as radiotherapy, i.e., particle therapy, and diagnosis like positron emission tomography (PET). However, the first priority is of course treatment of patients. Thus, exposure of medical staff working in such facilities is sometimes not so focused on. In the medical field, after stopping the radiological equipment such as a particle accelerator, the staff often enters the equipment area immediately where residual radiations still remain. In this case, they are exposed to gamma-rays emitted from many produced radioisotopes of various half-lives. It is thus important to estimate the dose in real-time and provide this information to the medical staff on the spot. Usually, when a medical staff enters a controlled area where radiological equipment is installed, they are supposed to bring a personal dosimeter and/or survey meter. However, the personal dosimeter cannot show the result in real-time and while the survey meter has this capability, it only shows the radiation dose. Some survey meters can show the pulse height spectrum as well. However, if many kinds of radioisotopes are produced and the emitted gamma-ray energies are high, the obtained pulse height spectrum can no longer visualize the real energy spectrum. If the medical staff could see and recognize the energy spectrum and dose of gamma-rays at the same time in real-time, it could make them think about their own exposure doses more carefully and encourage them to understand the radiation risk in the medical field and finally lead to reduction of their exposure.

So far, real time measurement of pulse height spectra could be realized by using a portable gamma-ray spectrometer (Mount Sopris Instruments, 2018, for instance), which is sometimes used in nuclear inspections. However, such a survey meter can only show the pulse height spectrum, not the energy spectrum. It is difficult to measure and display an energy spectrum in real-time, because it normally requires a certain mathematical process (solution of inverse problem) and until now it has been carried out after the measurement.

In this study, we aim at providing information to the medical staff, of how many energetic gamma-rays exist and how strongly they are exposed to them. To achieve this, we have been developing a prototype monitor combined with a CsI scintillator and MPPC (Kobayashi et al., 2017a, 2017b), that can simultaneously measure the energy spectrum and dose of gamma-rays in real time. Until now, using standard gamma-ray sources, we confirmed the basic performance in terms of intrinsic efficiency and energy resolution, and discussed the possibility of real-time measurement (Nishimura et al., 2022). The present monitor requires real-time data deduction, for which we employed the Bayesian estimation with α method (Iwasaki, 1997). With this method, the real-time estimation was basically realized so far by the authors' group, however, there is a severe problem left, i.e., the convergence speed was

* Corresponding author.
E-mail address: murata@see.eng.osaka-u.ac.jp (I. Murata).

https://doi.org/10.1016/j.apradiso.2024.111454
Received 4 June 2021; Received in revised form 12 February 2024; Accepted 23 July 2024
Available online 24 July 2024

very slow. In additionwhen the α value was larger, the convergence was unstable, although a larger α value is necessary to speed up the convergence. In the present study to solve these problems, a new Bayesian estimation scheme, *k*-α, is proposed. With this scheme, the convergence can be appropriately controlled. In the following chapters, the theory is detailed and experimental validation with standard gamma-ray sources is described.

2. Bayesian estimation

Iwasaki introduced Bayes' theorem to solve the inverse problem in radiation measurement [(Iwasaki, 1997)]. The Bayesian estimation consists of two processes named spectrum type and sequential type. The spectrum type Bayesian estimation is utilized in common radiation measurements [(Kondo et al., 2011; Takagi and Murata, 2016; Tamaki et al., 2017)]. This estimation is basically a post-process procedure, meaning that the data deduction is carried out after the measurement. In the present monitor, the sequential Bayesian estimation was thus employed, because the present monitor estimates gamma-ray energy spectrum in real-time, i.e., count by count. At first, a brief description is given for the Bayesian estimation.

There is a quantitative relationship between energy spectrum ϕ_j ($j = 1\sim n$) and measured pulse height spectrum y_i ($i = 1\sim m$) using a detector response function matrix, R_{ij}, which includes information about the detector dependent detection efficiency for gamma-ray energy. This relationship can explicitly be expressed by the next equation.

$$y_i = \sum R_{ij}\phi_j \tag{1}$$

To estimate the energy spectrum ϕ_j by solving this equation is generally called inverse problem, and the process of finding the energy spectrum is called *unfolding* in radiation measurement (Bouchet, 1995; Amadè et al., 2020). However, this task is not straightforward, because in radiation measurement equal relation, " = ", in Eq. (1) does not hold in most cases. We thus need to solve the equation not mathematically but from an engineering point of view.

According to the Bayes' theorem [(Iwasaki, 1997)], when one radiation is counted by a detector at pulse height channel *i*, the posterior probability of the energy spectrum at *j*, $P(j|i)$, can be derived by the response function R_{ij} of the detector and the energy spectrum ϕ_j as shown in the next equation (Kobayashi et al., 2017a).

$$P(j|i) = \frac{R_{ij}\phi_j}{\sum_{j=1}^{n} R_{ij}\phi_j} \tag{2}$$

In the spectrum type Bayesian estimation, unfolding is performed by multiplying this conditional probability by the count y_i and summing up. This process is conducted repeatedly to estimate ϕ_j with the following equation.

$$\phi_j^{(k+1)} = \sum_{i=1}^{m}\left(y_i \cdot \frac{R_{ij}\cdot\phi_j^{(k)}}{\sum\limits_{j=1}^{n} R_{ij}\cdot\phi_j^{(k)}}\right), \tag{3}$$

where $\phi_j^{(k)}$ is *k*-th estimation of ϕ_j.

This process is carried out after the whole measurement is completed. In the spectrum type Bayesian estimation, an obtained posterior probability is used as the prior probability in the next estimation turn. This iteration calculation is performed until the estimation would converge. The convergence was precisely discussed by Nauchi and Iwasaki (2014), who showed that Eq. (3) could be converged in case of infinite statistics. In the present study, the sequential Bayesian estimation is used instead to continuously perform this unfolding process in real-time during the measurement. The sequential type is a method of revising the spectrum by adding the contribution for each new detected count at channel *i*, that can be expressed by Eq. (4).

$$\phi_j^{'} = \phi_j + \frac{R_{ij}\phi_j}{\sum_{j=1}^{n} R_{ij}\phi_j} \tag{4}$$

where ϕ_j is the estimated gamma-ray energy spectrum before the last count, and ϕ_j' is the energy spectrum revised by the presently detected count.

With this equation, measurement in real-time becomes possible in principle. However, in real applications it is not so straightforward, because the convergence is known to be very slow. In this research, α method proposed by Iwasaki (1997) described in Eq. (5) was employed to accelerate the convergence speed. However, it was also known that it would be somewhat difficult to set an appropriate α value ($0 < \alpha < 1$) suitable for each inverse problem. The value α is interpreted as an index which can control how strongly the prior probability affects the posterior probability.

$$\phi_j' = (1-\alpha)\phi_j + \alpha\frac{R_{ij}\phi_j}{\sum_{j=1}^{n} R_{ij}\phi_j} \tag{5}$$

As described earlier, there are very few examples with the sequential Bayesian estimation, because the convergence is still slow for real applications, in addition to the difficulty of the α value setting. In the present study, the sequential Bayesian estimation with α method is improved to further speed up the convergence.

3. Measurement with α method

The authors' group carried out experimental studies so far with our own prototype monitor to estimate the gamma-ray energy spectrum with the α method [Kobayashi et al., 2017a, 2017b]. It was found from the result that the estimation was successful, however the convergence was not satisfactory. In the present study, precise experiments with standard gamma-ray sources were carried out once again to elucidate the problem we should solve.

3.1. Prototype monitor (Kobayashi et al., 2017a, 2017b)

The present monitor focuses on utilization in medical fields such as in hospitals. The following four design requirements were thus taken into account.

3.1.1. Small and light

Medical staffs normally enter an irradiation room after stopping the radiological equipment such as an accelerator. The staff needs to be able to enter the room and see the patient as soon as possible while also being aware of the dose exposure. So having a small and light monitor, that can be carried with ease, will not disturb their work.

3.1.2. High detection efficiency and good energy resolution

It is necessary to select a detection element which has a good detection efficiency so that a clear photo peak can be formed in the response function, and it should possess a good energy resolution to visually distinguish photo peaks so as to understand the energy spectrum clearly and correctly.

3.1.3. No hygroscopicity

In order to reduce the size and weight and for the producibility of the monitor, it is desirable that the detector has no hygroscopicity, since otherwise an airtight enclosure would be necessary. CsI(Tl) crystals are only very slightly hygroscopic and do not require such enclosure, as they deteriorate only when in contact with water or extremely high moisture (Knoll, 2010).

3.1.4. Upper gamma-ray energy of 3 MeV

The present monitor is designed to be used after stopping the radiological equipment like an accelerator. This means primary particles like protons, neutrons and so on do not exist when using the monitor. It is thus not necessary to take care of capture gamma-rays. Since only gamma-rays emitted via decay of radioisotopes produced by the primary particles exist, 3 MeV, which is the maximum energy of such gamma-rays, is appropriate as the upper energy limit of the monitor.

In addition to the above four conditions, following guidelines for portable radiation monitors and other commercial dosimeters developed for similar applications, we consider as a final goal a dose rate range between 0.05 μSv/h (background) and 10 mSv/h (IEC, 2009), while thinking of the current goal of background to 1 mSv/h for energies up to 3 MeV as described above.

To meet the above conditions, we chose a CsI scintillator as a detection device of gamma-rays. This is because the performance is more-or-less the same as or even better than the commonly used NaI scintillator and in addition, CsI has almost no hygroscopicity, unlike NaI. In recent years it has become possible to produce and utilize large CsI crystals in radiation detection. In this study, a cubic CsI (Tl) crystal of $2.6 \times 2.6 \times 2.6$ cm^3 (Fig. 1) supplied by I.S.C. Lab.(I.S.C. Lab, 2011) was employed for the prototype monitor. Although this size is not finally fixed, from the preliminary design study it was confirmed to be acceptably large to estimate doses even in background circumstances. Also, in order to reduce the weight, we decided to combine the CsI crystal with a multi-pixel photon counter (MPPC) (Hamamatsu Photonics K. K, 2019] shown in Fig. 2 instead of a normally used photo-multiplier tube (PMT). Fig. 3 shows the light and small prototype monitor we developed.

3.2. Measurement with standard gamma-ray sources

Measurements were carried out with the prototype monitor described in Sec. 3.1. The real-time measurements were virtually carried out by sampling each count from the population, which was obtained by a long-time measurement. This is important for reproducibility,

Fig. 1. CsI(Tl) scintillator ($2.6 \times 2.6 \times 2.6$ cm^3). [I.S.C. Lab, 2011].

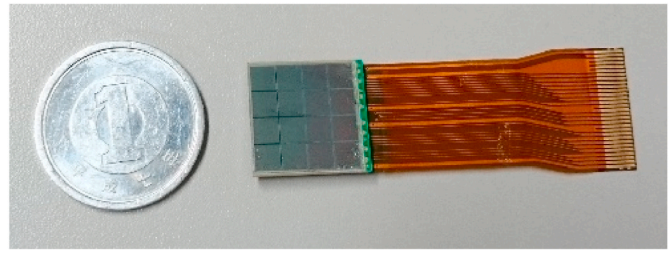

Fig. 2. Multi-pixel photon counter (MPPC). [Hamamatsu Photonics K. K, 2019].

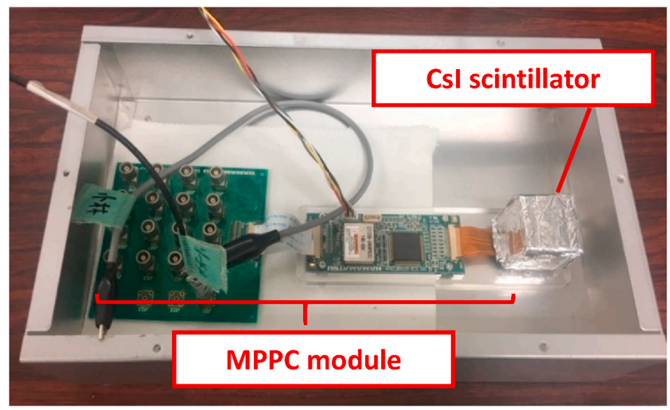

Fig. 3. Developed prototype monitor [Kobayashi et al., 2017a; 2017b].

meaning that it is valuable for debugging the data deduction system. As gamma-ray sources, initially standard gamma-ray sources were considered to be used, however, they are normally mono-energetic. Thus in the present study, several sources of ^{133}Ba, ^{137}Cs and ^{60}Co, were combined and an experimental radiation field was formed to simulate real conditions as closely as possible. The details of the sources are summarized in Table 1. Fig. 4 shows the schematic of the experimental system. The gamma-ray sources were placed at 18 cm from the prototype monitor, which was set on a 1 cm thick aluminum plate. The dose rate at the monitor position is around 6 μSv/h. Fig. 5 shows an example of the measured pulse height spectrum by the monitor at 600 s. The count rate and the total number of counts are 1500 counts/sec (cps) and 9.01x 10^5 counts, respectively. Fig. 6 shows the estimated gamma-ray energy spectra for $\alpha = 10^{-2}$, 10^{-3} and 10^{-4} at 30 s. For $\alpha = 10^{-2}$, the energy spectrum shape seems to be reproduced; however, it is really unstable especially for the absolute values. For example, this is evident from the fact that the two large peaks of ^{60}Co do not agree with each other. However, thistrend is improved with the decrease of α value. For the case of $\alpha = 10^{-4}$, however, the energy spectrum seems to not yet converge compared to $\alpha = 10^{-3}$. Fig. 7 shows the results of 300 s for $\alpha = 10^{-3}$ and 10^{-4}. The estimated energy spectrum is found to be improved with an increase in measuring time. The same performance as the case

Table 1
Gamma-ray sources used[a1].

Nuclide	Half life (year)	Gamma-ray energy (keV)	Intensity per decay (%)
133Ba	10.5	81	34
		276	7
		303	18
		356	62
		384	9
137Cs	30	662	85
60Co	5.3	1173	100
		1332	100

[a] 1 Cited from [Firestone and Shirley, 1996].

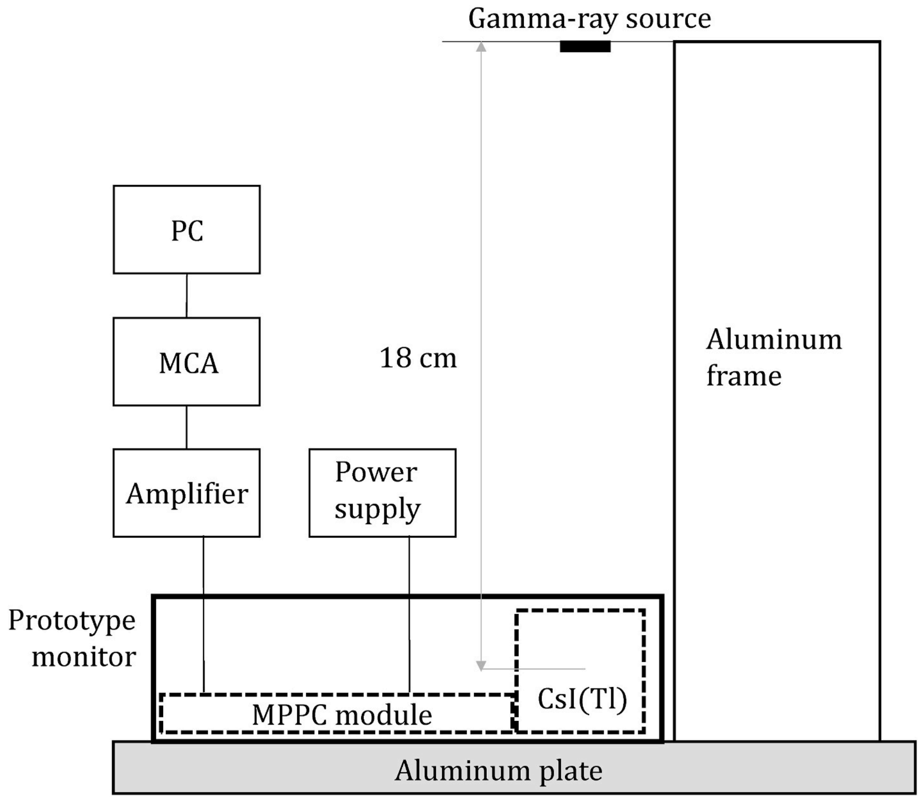

Fig. 4. Schematic of the experimental system.

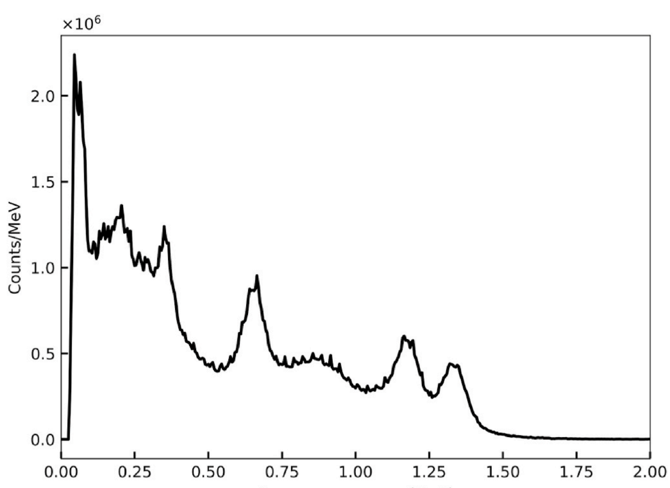

Fig. 5. Pulse height spectrum measured by the prototype monitor for 600 s with ^{133}Ba, ^{137}Cs and ^{60}Co.

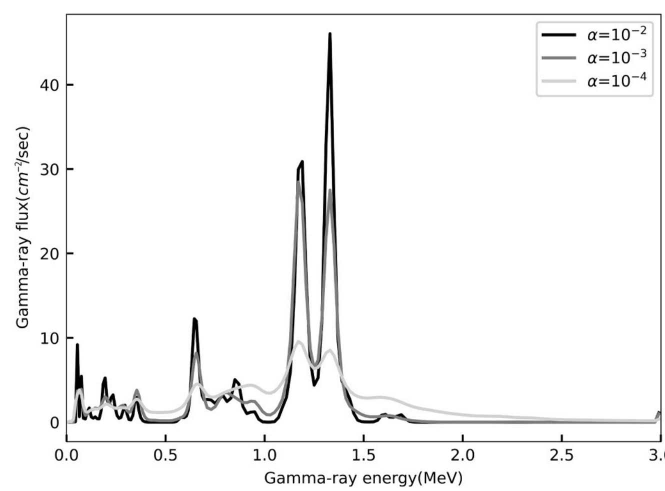

Fig. 6. Estimated gamma-ray energy spectra at 30 s ($\alpha = 10^{-2}$, 10^{-3} and 10^{-4}).

for 30 s and $\alpha = 10^{-3}$ in Fig. 6 is obtained in the case of 300 s and $\alpha = 10^{-4}$. Comparing the result of $\alpha = 10^{-3}$ and 10^{-4} at 300 s, the convergence of both cases of $\alpha = 10^{-3}$ and 10^{-4} seems acceptable. From the result, it was confirmed that by adjusting the α value appropriately, an acceptably converged energy spectrum can be obtained in several tens of seconds.

Kondo pointed out inhis spectrum type Bayesian estimation study [Kondo, 2008] that over-revision (a moderately unstable result) is observed with an increase of the iteration number using Eq. (3), and also noted that this is probably a feature characteristic of Bayesian estimation. In the sequential Bayesian estimation this phenomenon is equivalent to the situation where the number of counts increases or α is large. In the present results, the unstable result of $\alpha = 10^{-2}$ may thus be due to the over-revision. In the case of $\alpha = 10^{-3}$, over-revision was not observed from Fig. 7. In summary, in the present measuring circumstances, we concluded that this phenomenon was not observed if $\alpha \leqq 10^{-3}$, and we believe it can be ignored in the present monitor, because the measuring time is normally not so long in medical application spots.

Fig. 8 shows doses derived from the estimated energy spectrum and the flux-to-dose conversion coefficient [Atomic Energy Society of Japan, 2010] in real-time as a function of measuring time. The horizontal solid line is the theoretical value, which is calculated with the effective dose rate constant [Japan Radioisotope Association, 2009]. The presently measured values are in good agreement with the theoretical value. In addition, the present results were compared with that of an NaI scintillation survey meter (Hitachi Aloka Medical, 2010) measured at the

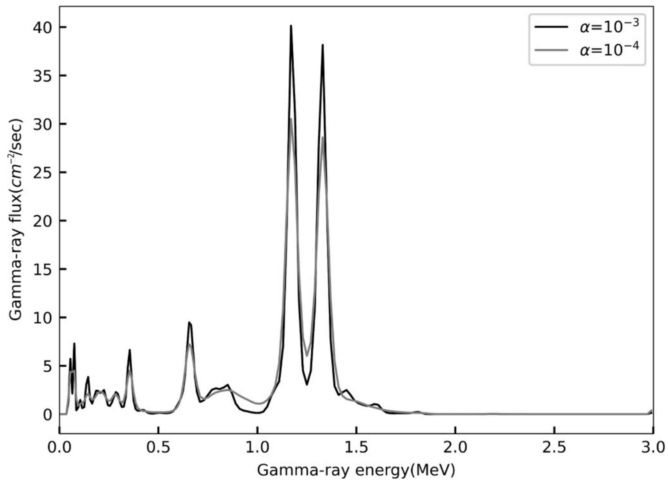

Fig. 7. Estimated gamma-ray energy spectra at 300 s ($\alpha = 10^{-3}$ and 10^{-4}).

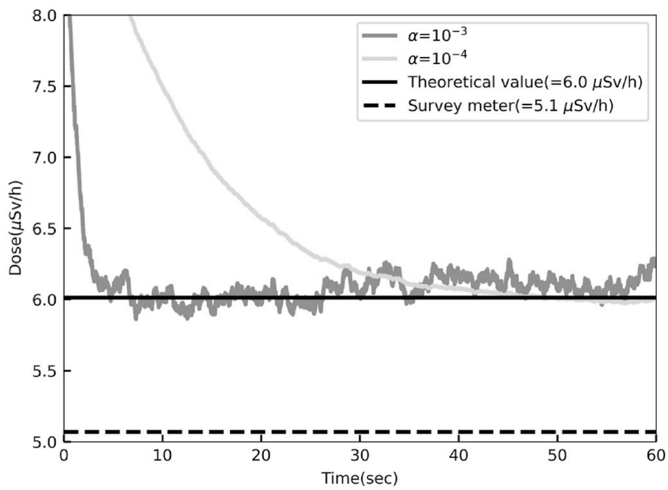

Fig. 8. Estimated doses ($\alpha = 10^{-3}$ and 10^{-4}) compared with theoretical and survey meter values.

same position, which is represented as a dashed line. The error of the readings of the survey meter was 11%. This discrepancy will be discussed in Sec. 4.3.

Regarding the convergence performance, for $\alpha = 10^{-2}$, the estimated value converges from the beginning, however, the value is critically unstable. In order to converge, it requires ~5 s for $\alpha = 10^{-3}$ and ~40 s for $\alpha = 10^{-4}$. Considering practical applications, the accuracy for $\alpha = 10^{-2}$ is poor. In the case of $\alpha = 10^{-3}$ the accuracy is fairly well, however, there is more fluctuation observed when compared to that of $\alpha = 10^{-4}$, for example, at 40 s. For α less than 10^{-4} the accuracy is acceptable, however, the convergence may be a little slow for practical use.

4. *k*-α method

4.1. Principle of the method

In α method, revision is performed when a count is detected. If $\alpha = 10^{-2}$, one percent of the total flux is revised by one count detection, meaning after 100 counts (=1/α), 100 percent (named one round in this paper) of a revision is completed. After several rounds of iterations, the revision proceeds well and finally the convergence is achieved. In the case of $\alpha = 10^{-4}$, however, one round requires 10000 counts. It takes time to reach one round compared to the case of $\alpha = 10^{-2}$. This is the cause of deterioration of the convergence speed. This suggests setting larger α value allows for faster convergence. However, as described in Chap. 3, if employing a larger α value, the convergence is surely very fast, however, the result becomes unstable. In practical applications, α value should be set appropriately, i.e., sometimes it should be set smaller and sometimes larger so that the revision proceeds properly. This indicates that the convergence speed can change depending on the count rate. If the count rate is high, α value should be smaller. This means that there may exist a suitable α value for each measurement condition. As discussed in Chap. 3, α values less than 10^{-3} seem to be preferable, however, the convergence speed may be slow in case of $\alpha = 10^{-4}$. In the present study, for practical applications, the possibility of continuous change of α value during measurement is examined.

The simplest way to achieve this is by setting $\alpha = 1/N$, where N is the number of counts. In this case, for example in the second count, α becomes 0.5 and the revision proceeds by 50%, and in the third count, $\alpha = 0.33$ and the revision is 33%. At N-th count, the revision ratio is $1/N$. Seemingly $\alpha = 1/N$ is acceptable. However, if N becomes very large, the result is not revised any more, because for example in the case of 1 million counts, $\alpha = 10^{-6}$ and the revision ratio is just 0.001%. It is really not practical, because the α value is too small.

In this study, therefore, at first α value decreases as $1/N$. And, finally we control it as it is approaching a certain small value. Practically, α value is made to change continuously according to the next equation.

$$\alpha = \frac{1 + kN}{N} \left(\alpha = 1 \text{、 if } N < \frac{1}{1 - k} \right), \tag{6}$$

where k is the convergence control factor ($0 < k < 1$). This revision procedure with Eq. (6) is called k-α method in this paper. This can accelerate the convergence of revision, suppressing unwanted decrease of α value. Change of α for the number of counts, N, is shown in Fig. 9. It is found that α value converges to k with increase of N. The α value convergence can be found at $N > 1/k$. Consequently, Eq. (5) is revised as below.

$$\phi_j^{'} = \frac{(1-k)N - 1}{N}\phi_j + \frac{1 + kN}{N} \bullet \frac{R_{ij}\phi_j}{\sum_{j=1}^{n} R_{ij}\phi_j} \tag{7}$$

4.2. Unfolding with *k*-α method

To validate the k-α method, unfolding was carried out with Eq. (7) using the same experimental data as in Sec. 3.2. As a result, for the energy spectrum, similar to α method, the reproducibility became stable with decrease of α value. Also, the convergence of the estimated energy spectrum was improved with measuring time. As an example, Fig. 10 shows the result at 300 s for $k = 10^{-4}$, which corresponds to $\alpha = 10^{-4}$, because $\alpha \cong k$, if $N \rightarrow \infty$. Both results show an acceptable and similar

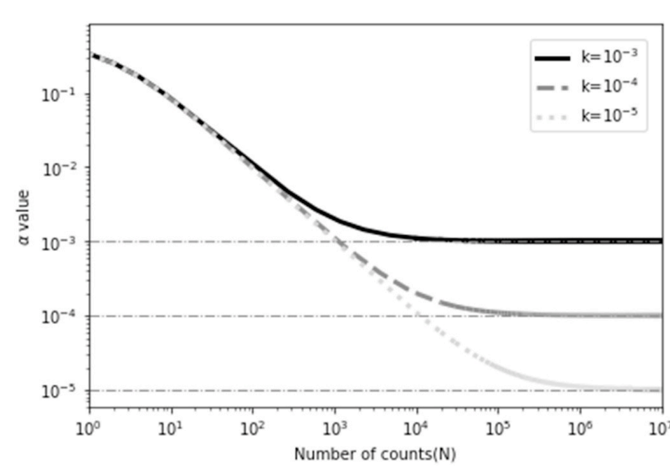

Fig. 9. α Value change for the number of counts, N ($k = 10^{-3}$, 10^{-4} and 10^{-5}).

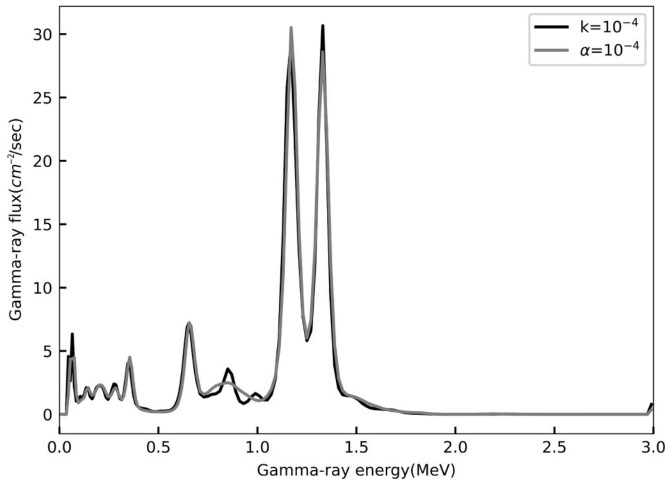

Fig. 10. Estimated gamma-ray energy spectra at 300 s ($k = 10^{-3}$, $\alpha = 10^{-3}$).

performance at 300 s. This trend is observed in case of other elapsed time.

Detailed discussion of the performance of k-α method is carried out in dose estimation results as below, since the quantitative discussion is more straightforward compared to the energy spectrum. This is because dose is an integral value of the energy spectrum. Dose rates were estimated with the obtained energy spectra and the flux-to-dose conversion coefficient [Atomic Energy Society of Japan, 2010)]. Fig. 11 shows the results of the cases of $k = 10^{-3}$, 10^{-4} and 10^{-5}, respectively. The case of $k = 10^{-2}$ is not described, because it showed critical instability. For the other cases, the dose convergence is fast compared to α method as shown in Fig. 8. For $k = 10^{-3}$ a slightly larger instability can be observed, leading to the conclusion that $k \leqq 10^{-4}$ is preferable. More practically, compared to the α method, when $k = 10^{-4}$, the approach to the theoretical value is faster than in the case of $\alpha = 10^{-4}$. If k is set to a very small value, the number of counts required for one round ($1/k$) is too large to revise the dose appropriately. This trend is the same for the α method. This is concretely observed in the case of $k = 10^{-5}$, where the approaching speed to the theoretical value is slower in this time range compared to the case of $k = 10^{-4}$, and as a result the agreement with the theoretical value is not sufficient. Conversely, this means that longer measuring time could improve the agreement. From the above discussion it is understood that the setting of k has a significant relation to count rate, and by extension the dose rate. In other words, we need to set

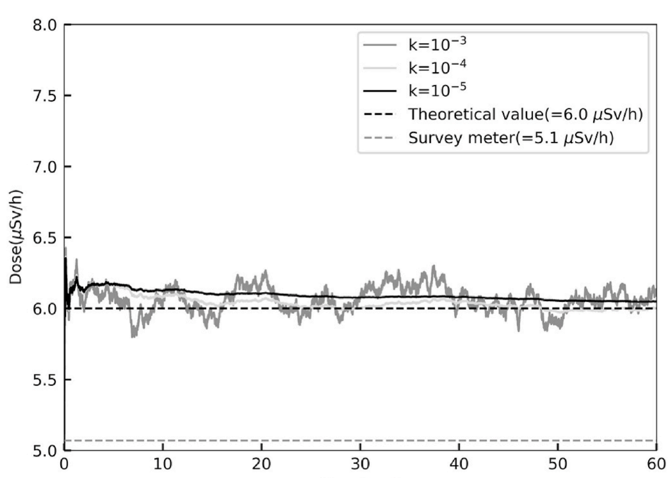

Fig. 11. Estimated doses ($k = 10^{-3}$, 10^{-4} and 10^{-5}) compared with theoretical value.

the k value while considering the radiation intensity at the measurement location.

In conclusion, under the present measuring conditions of around 6 μSv/h, using the k-α method ($\alpha = 10^{-4}$) a stable and accurate dose value can be displayed almost from the beginning of measurement, within a few seconds, and at the same time the energy spectrum can be shown correctly within several tens of seconds. Finally, using the present monitor even in a medical application where the spectrum is unknown, the value of k can be quickly adjusted according to the count rate, ensuring accurate measurements. Recently, in the author's laboratory, measurements in front of a nuclear fuel storage room (~2 μSv/h) and the weakest radiation field of background, have been carried out in order to investigate the effectiveness of the monitor in a field with a complex gamma-ray spectrum(Nishimura et al., 2022).

4.3. *Comparison with survey meter values*

As described in Secs. 3.2 and 4.2, for both α and k-α methods, the estimated dose values differ from the survey meter value beyond the measurement error. The reason for this discrepancy will be discussed in the present chapter. Table 2 shows a dose comparison, with standard gamma-ray sources of ^{133}Ba, ^{137}Cs and ^{60}Co, between the k-α method ($k = 10^{-4}$), survey meter and theoretical value. The measuring conditions and procedure are the same as Sec. 3.2. From the table, doses for ^{137}Cs show an equal value among the three measurements as expected. However, for the other two sources an excellent agreement is seen between k-α method and the theoretical calculation, but a discrepancy is found for k-α method (and theoretical values) and the survey meter values. The reason for this is the fact that the survey meter is calibrated with a standard radiation source, i.e., ^{137}Cs, wheras in the k-α method the dose is estimated exactly with the measured gamma-ray energy spectrum and the flux-to-dose conversion coefficient. More practically, as listed in Table 2, the conversion coefficient of ^{60}Co is larger than ^{137}Cs and that of ^{133}Ba is smaller than ^{137}Cs, and the total of the three contributions should be summed to estimate the total dose, if using the three sources together. In the present case, the ^{60}Co source is dominant, indicating that the survey meter values shown are lower.

With this monitor, as described earlier, the dose can be estimated accurately from the obtained energy spectrum and the flux-to-dose conversion coefficient. This means that even when the energy distribution is complicated or the energy is high, dose estimation can be performed successfully and with precision. This is one of the remarkable and advantageous features of the present monitor.

5. Conclusion

We have been developing a small and light monitor for the medical staff in medical application spots after switching-off radiological equipment. The monitor can display the gamma-ray energy spectrum and dose at the same time in real-time. A prototype monitor was developed, and measurements were conducted with standard gamma-

Table 2
Comparison of doses for the present method, theoretical and survey meter values.

	^{133}Ba			^{137}Cs	^{60}Co	
Strongest three gamma-ray energies (keV)	356	81	303	662	1173	1332
Intensity per decay (%)	62	34	18	85	100	100
Flux-to-dose conversion coefficient[a]1 (pSv・cm2)	1.78	0.44	1.52	3.17	5.04	5.54
Survey meter	0.27			0.57	4.23	
Theoretical value	0.16			0.567	5.3	
Bayesian estimation	0.165			0.569	5.28	

[a] 1 Cited from [Atomic Energy Society of Japan, 2010].

ray sources of ^{133}Ba, ^{137}Cs and ^{60}Co to test the monitor's performance. The sequential Bayesian estimation method was employed and a new scheme, *k*-α, was proposed for the real-time measurement by improving the conventional α method to accelerate the convergence. With this monitor, the gamma-ray dose can be measured and displayed almost from the beginning of measurement, at least within several seconds, for $\alpha = 10^{-4}$ in the measurement conditions of around 6 μSv/h. It can also show the energy spectrum simultaneously within several tens of seconds.

CRediT authorship contribution statement

Isao Murata: Conceptualization, Funding acquisition, Methodology, Project administration, Writing – original draft. **Nikolaos Voulgaris:** Data curation, Investigation, Software, Writing – review & editing. **Takaaki Miyoshi:** Investigation, Software, Validation, Visualization. **Moe Shinohara:** Conceptualization, Methodology, Writing – original draft. **Hikari Nishimura:** Formal analysis, Investigation, Validation. **Mina Kobayashi:** Conceptualization, Investigation, Methodology. **Sachie Kusaka:** Data curation, Project administration, Visualization, Writing – review & editing. **Shingo Tamaki:** Project administration, Validation, Writing – review & editing. **Fuminobu Sato:** Conceptualization, Validation, Writing – review & editing.

Declaration of competing interest

We have no conflict of interest for the contents in this paper.

Data availability

Data will be made available on request.

References

Amadè, S., Bettelli, N., Zambelli, N., Zanettini, S., Benassi, G., Zappettini, A., 2020. Gamma-ray spectral unfolding of CdZnTe-based detectors using a genetic algorithm. Sensors 20 (24), 7316. https://doi.org/10.3390/s20247316.

Atomic Energy Society of Japan, 2010. Dose Conversion Factor for Radiation Shielding Calculation, p. 2010. AESJ-SC-R002:2010).

Bouchet, L., 1995. A comparative study of deconvolution methods for gamma-ray spectra. Astron. AstroPhys. Suppl. 113, 167–183.

Firestone, R.B., Shirley, V.S. (Eds.), 1996. Table of Isotopes, eighth ed. John Wiley & Sons, Inc.

Hamamatsu Photonics K. K., 2019. https://www.hamamatsu.com/jp/en/index.html (May 7, 2019 accessed).

Hitachi Aloka Medical, 2010. Merged into Hitachi Ltd, vol. 2011. http://www.hitachi.com/businesses/healthcare/index.html.

International Electrotechnical Commission (IEC), 2009. Radiation protection instrumentation – ambient and/or directional dose equivalent (rate) meters and/or monitors for beta. X and Gamma Radiation – Part 1: Portable Workplace and Environmental Meters and Monitors. IEC 60846-1, Edition 1.0, 2009-04.

I.S.C. Lab., 2011. http://www.isc-lab.com/index.html (in Japanese, May 7, 2019 accessed).

Iwasaki, S., 1997. A new approach for unfolding problems based only on the Bayes' Theorem. Proceedings of the 9th International Symposium on Reactor Dosimetry, pp. 245–252.

Knoll, G.F., 2010. Radiation Detection and Measurement, fourth ed. Wiley, Hoboken, N. J, pp. 241–242.

Kobayashi, M., Sato, F., Kusaka, S., Murata, I., 2017a. Feasibility study on real-time γ-ray spectrum/dose measurement system. EPJ Web Conf. 153, 07014, 6pp.

Kobayashi, M., Sato, F., Murata, I., 2017b. Feasibility study on real-time γ-ray spectrum/dose measurement system. Trans. Am. Nucl. Soc. 116, 985–998.

Kondo, K., 2008. Experimental Studies on Fusion Neutron-Induced Charged-Particle Emission Reactions of Light Elements. Osaka University. Doctor dissertation.

Kondo, K., Murata, I., Ochiai, K., Kubota, N., Miyamaru, H., Konno, C., Nishitani, T., 2011. Measurement of charged-particle emission double-differential cross section of fluorine for 14.2 MeV neutrons. J. Nucl. Sci. Technol. 48 (8), 1146–1157.

Mount Sopris Instruments, 2018. RS-330 Series Portable Gamma Ray Spectrometer. https://mountsopris.com/rs-330-series-portable-gamma-ray-spectrometer/. (Accessed 1 April 2020).

Nauchi, Y., Iwasaki, S., 2014. Convergence of unfolded spectrum with response function for single radiation based on Bayes' theorem. Nucl. Instrum. Methods A735, 437–443.

Nishimura, H., Shinohara, M., Miyoshi, T., Voulgaris, N., Kusaka, S., Tamaki, S., Sato, F., Murata, I., 2022. Experimental verification of real-time gamma-ray spectrum and dose monitor. Appl. Radiat. Isot. 185, 110226 https://doi.org/10.1016/j.apradiso.2022.110226.

Takagi, H., Murata, I., 2016. Development of precise energy spectrum measurement technique for high-power pulsed X-ray sources for industrial use. J. Nucl. Sci. Technol. (Tokyo, Jpn.) 53 (6), 766–773.

Tamaki, S., Sato, F., Murata, I., 2017. Study on a liquid-moderator-based neutron spectrometer for BNCT – development and experimental test of the prototype spectrometer. Nucl. Instrum. Methods A870, 90–96.

Japan Radioisotope Association, 2009. Radioisotope pocket data book. Maruzen (in Japanese), 20.